Guan Xin Dan Shen formulation protects *db/db* mice against diabetic cardiomyopathy via activation of Nrf2 signaling

BIN ZHANG, CHEN-YANG ZHANG, XUE-LIAN ZHANG, GUI-BO SUN and XIAO-BO SUN

Institute of Medicinal Plant Development, Peking Union Medical College and
Chinese Academy of Medical Sciences, Beijing 100193, P.R. China

Abstract. Guan Xin Dan Shen formulation (GXDSF) is a widely used treatment for the management of coronary heart disease in China and is composed of three primary components: *Dalbergiae odoriferae* Lignum, *Salviae miltiorrhizae* Radix et Rhizoma and *Panax notoginseng* Radix et Rhizoma. However, the potential use of GXDSF for the management of diabetic cardiomyopathy (DCM) has not been previously assessed. The present study aimed to assess the effects of GXDSF on DCM, as well as the underlying mechanism. In the present study, *db/db* mice were used. Following treatment with GXDSF for 10 weeks, fasting blood glucose, insulin sensitivity, serum lipid levels and cardiac enzyme levels were detected. Cardiac pathological alterations and cardiac function were assessed by performing hematoxylin and eosin staining and echocardiograms, respectively. TUNEL assays were conducted to assess cardiomyocyte apoptosis. Additionally, reverse transcription-quantitative PCR and western blotting were performed to evaluate the expression of apoptosis-associated genes and proteins, respectively. In the model group, the *db/db* mice displayed obesity, hyperlipidemia and hyperglycemia, accompanied by noticeable myocardial hypertrophy and diastolic dysfunction. Following treatment with GXDSF for 10 weeks, serum triglyceride levels were lower and insulin sensitivity was enhanced in *db/db* mice compared with the model group, which indicated improvement in condition. Cardiac hypertrophy and dysfunction were also improved in *db/db* mice following treatment with GXDSF, resulting in significantly increased left ventricular ejection fraction and fractional shortening compared with the model group. Following treatment with metformin or GXDSF, model-induced increases in levels of myocardial enzymes were decreased in the moderate and high dose groups. Moreover, the results indicated that, compared with the model group, GXDSF significantly inhibited cardiomyocyte apoptosis in diabetic heart tissues by increasing Bcl-2 expression and decreasing the expression levels of Bax, cleaved caspase-3 and cleaved caspase-9. Mechanistically, GXDSF enhanced Akt phosphorylation, which upregulated antioxidant enzymes mediated by nuclear factor erythroid 2-related factor 2 (Nrf2) signaling. Collectively, the results of the present study indicated that GXDSF attenuated cardiac dysfunction and inhibited cardiomyocyte apoptosis in diabetic mice via activation of Akt/Nrf2 signaling. Therefore, GXDSF may serve as a potential therapeutic agent for the management of DCM.

Introduction

Diabetes mellitus (DM) is a major public health concern globally. In 2015, there were 415 million diabetic patients in total and it is estimated that this will increase to 642 million by 2040 (1). Despite notable progress in the management of blood glucose in diabetic patients (2), the complications of diabetes are often the cause of death in affected patients, and the clinically available strategies for the management of complications of diabetes are limited (3).

Diabetic cardiomyopathy (DCM) is a common macrovascular complication that is characterized by ventricular hypertrophy, heart failure and cardiac fibrosis (4-6). Increasing evidence has demonstrated that, in addition to chronic inflammation, mitochondrial dysfunction and oxidative stress also contribute to the development of DCM (7-9). Although certain therapies, including zinc supplementation (10), advanced glycation end product breakers (aminoguanidine) (11), copper chelators (trientine) (12), metformin (13,14), angiotensin-converting enzyme inhibitors (15,16), β-blockers (timolol) (17) and dipeptidyl peptidase-4 inhibitors (18), have been assessed in animal studies, none of these therapies have been reported to be effective in patients with DCM due to their side effects, and the underlying mechanisms of action in the modulation of DCM are not completely understood.

The nuclear factor erythroid 2-related factor 2 (Nrf2) signaling pathway is crucial for the regulation of endogenous

Correspondence to: Professor Xiao-Bo Sun or Professor Gui-Bo Sun, Institute of Medicinal Plant Development, Peking Union Medical College and Chinese Academy of Medical Sciences, 151 Malianwa North Road, Haidian, Beijing 100193, P.R. China
E-mail: sun-xiaobo@163.com
E-mail: sunguibo@126.com

antioxidant enzyme protein expression levels (19), including heme oxygenase-1 (HO-1) and γ-glutamylcysteine synthetase heavy subunit (γ-GCS). Nrf2-mediated antioxidant enzymes are closely associated with inhibition of oxidative stress and protection against DCM (20,21). Therefore, enhancement of Nrf2 signaling may serve as a promising therapeutic strategy for preventing the development of DCM.

The Guan Xin Dan Shen formulation (GXDSF) is primarily composed of *Panax notoginseng* Radix et Rhizoma, *Dalbergiae odoriferae* Lignum and *Salviae miltiorrhizae* Radix et Rhizoma, and is a herbal prescription of Traditional Chinese Medicine (22). GXDSF has been used clinically for the treatment of cardiovascular diseases (23). Our previous study demonstrated that GXDSF prevented left ventricular remodeling induced by myocardial ischemia/reperfusion injury (22). High-performance liquid chromatography (HPLC) has been used to identify the contents of the chemical components of GXDSF, demonstrating that it is composed of notoginsenoside R1 (2.34%), ginsenoside Rb1 (8.63%), salvianolic acid B (0.50%), ginsenoside Rg1 (9.51%), crypto-tanshinone (0.84%), tanshinone I (0.55%) and tanshinone IIA (1.71%) (22). The key components have been reported to exert cardioprotective effects, including protecting against ischemia in rats following acute myocardial infarction (24), preventing cardiac hypertrophy in ApoE$^{-/-}$ mice (25) and attenuating high glucose-induced endothelial cell injury (26,27). Ginsenoside Rg1 ameliorates DCM by inhibiting endoplasmic reticulum stress (28). However, to the best of our knowledge, no previous studies have assessed the protective roles of GXDSF in DCM. Furthermore, the drugs currently available for the management of DCM are limited and are often accompanied by adverse effects (29). Therefore, assessing the protective effects of GXDSF in DCM is important.

In the present study, *db/db* mice were used to investigate whether GXDSF exerted a protective effect against DCM and to further determine the underlying mechanism.

Materials and methods

Drugs. Guan Xin Dan Shen dripping pills (40 mg/pill; cat. no. 20160426) were obtained from Harbin Pharmaceutical Group Co., Ltd. In our previous study, the aforementioned components of GXDSF were determined via HPLC (22). Metformin was provided by Sino-American Shanghai Squibb Pharmaceuticals, Ltd. Valsartan was provided by Novus Biologicals, Ltd.

Animals. Mice were obtained from GemPharmatech Co., Ltd. In total, 60 leptin receptor-deficient *db/db* 8-week-old male mice (weight, 40±2 g; BKS.Cg$^{+/+}$ Leprdb NJU) and 10 non-diabetic 8-week-old male mice (weight, 20±2 g; C57BLKS/J) were used in the present study. The mice were maintained at 22-24°C and 40% humidity with 12-h light/dark cycles and *ad libitum* access to food and water. All animal experiments were performed in accordance with the Guide for the Care and Use of Laboratory Animals (30). The present study was approved by the Laboratory Animal Ethics Committee of the Institute of Medicinal Plant Development, Peking Union Medical College and Chinese Academy of Medical Sciences (license no. SLXD-20190406017).

Groups and drug administration. After 4 weeks of acclimatization, the *db/db* mice were randomly divided into the following six groups (n=10 per group): i) *db/db* group (model); ii) *db/db* + metformin (140 mg/kg/day) group; iii) *db/db* + valsartan (48 mg/kg/day) group; iv) *db/db* + GXDSF high dose (180 mg/kg) group; v) *db/db* + GXDSF moderate dose (90 mg/kg) group; and vi) *db/db* + GXDSF low dose (45 mg/kg) group. The control group consisted of the C57BLKS/J mice (n=10). The clinic dose of GXDSF for patients with coronary heart disease is 20 mg/kg day. The doses of GXDSF used in the present study were based on the recommended clinical dose of GXDSF (31). Over a period of 10 weeks, the mice were administered drugs via gavage daily (Fig. 1A). Mice in the control and model groups were orally administered distilled water.

Fasting blood glucose (FBG) and insulin tolerance test (ITT) assay. The blood glucose of mice fasted overnight was measured using an automatic glucometer (Roche Diagnostics). For assessing insulin tolerance, an ITT assay was performed via intraperitoneal injection of 1 U/kg insulin (Sigma-Aldrich; Merck KGaA). The tail blood glucose concentration was measured every 30 min after injection for a total of 120 min, and is expressed as the area under the curve (AUC).

Echocardiography. Following treatment for 10 weeks, the mice were anesthetized with 1.2% avertin (300 mg/kg; intraperitoneal) and echocardiography was performed. The echocardiograms were obtained using a Vevo^{770} high-resolution imaging system (VisualSonics, Inc.). To calculate percentage ejection fraction (% EF) and percentage fractional shortening (% FS), M-mode tracing of the left ventricle (LV) based on the parasternal long-axis view was used. To evaluate left ventricular end diastolic diameter (LVIDd) and left ventricular end systolic diameter (LVIDs), the pulse-wave and tissue Doppler in mice at baseline and after treatment were used. LV end-diastolic volume (LVVd) and LV end-systolic volume (LVVs) were automatically calculated by an ultrasound machine (VisualSonics, Inc.).

Determination of serum lipids. After 10 weeks of treatment, the *db/db* mice were anesthetized using 4% chloral hydrate (400 mg/kg; intraperitoneal). Subsequently, ~0.75 ml blood was collected from the eye socket vein of mice fasted overnight. The anesthetized mice were then sacrificed via cervical dislocation. To obtain the serum samples, the blood was centrifuged at 3,000 x g for 15 min at room temperature. An automatic biochemical analysis system (Beckman Coulter, Inc.) was used to measure serum triglyceride (TG, cat. no. A110-1-1), low-density lipoprotein (LDL, cat. no. A113-1-1) and total cholesterol (TC, cat. no. A111-1-1) levels according to the manufacturer's protocol (Nanjing Jiancheng Bioengineering Institute).

Assessing myocardial enzyme activity. The serum myocardial enzyme activities of aspartate transaminase (AST; cat. no. C010-1-1), lactate dehydrogenase (LDH; cat. no. A020-1-2) and creatine kinase MB (CK-MB; cat. no. E006-1-1) were measured using specific detection kits (Nanjing Jiancheng Bioengineering Institute) according to the manufacturer's protocol.
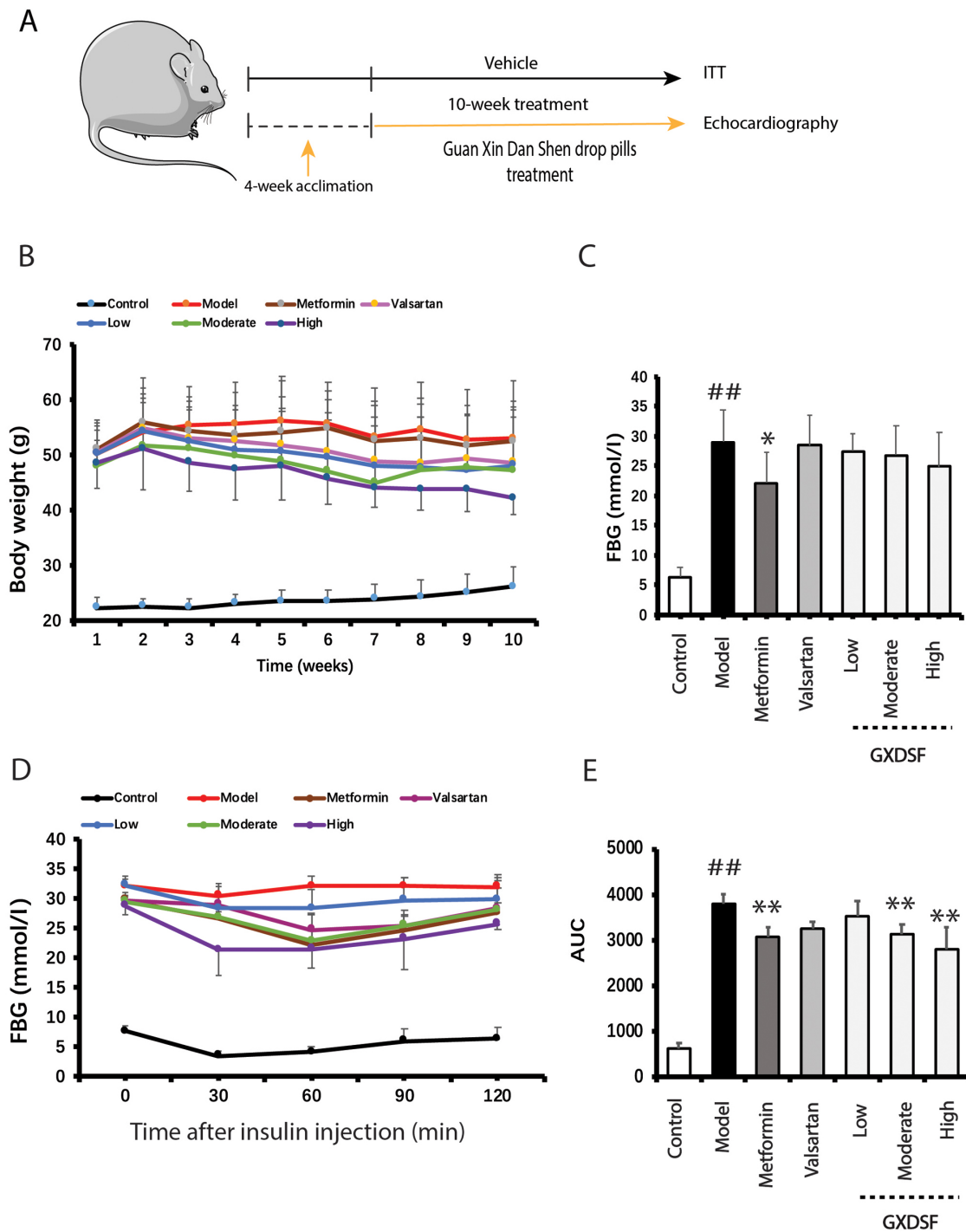
Figure 1. Effects of GXDSF on body weight and insulin sensitivity in *db/db* mice. (A) Schematic diagram indicating the timeline of the *in vivo* animal experiments. (B) Body weight and (C) fasting blood glucose levels in each group. Insulin sensitivity was evaluated by performing the intraperitoneal ITT and (D) quantified and (E) expressed as AUC. Data are represented as the mean ± SD (n=10). ##$P<0.01$ vs. control; *$P<0.05$ and **$P<0.01$ vs. model. GXDSF, Guan Xin Dan Shen formulation; ITT, insulin tolerance test; AUC, area under the curve; FBG, fasting blood glucose.

Histological analysis. After the mice were sacrificed, five heart tissue samples in each group were fixed in 4% buffered paraformaldehyde for 48 h at room temperature. Following embedding in paraffin, tissues were cut into 4-μm sections. Subsequently, sections were stained with hematoxylin and eosin (H&E) at room temperature as previously (32). Stained sections were examined by a blinded pathologist using a BX53 light microscope (Olympus Corporation; magnification, x200).

TUNEL staining. The aforementioned fixed and embedded heart samples were cut into 4-μm sections and then deparaffinized using xylene. The antigen retrieval was performed by heating the tissues to 80°C. Subsequently, the sections were incubated with Protease K for 15 min at room temperature before pre-incubation with terminal deoxynucleotidyl transferase buffer (Sigma-Aldrich; Merck KGaA) at 37°C for 60 min. After washing with PBS, the sections were incubated with an anti-digoxin and anti-serum alkaline phosphatase

Table I. Sequences of primers used for quantitative PCR.

Gene	Sequence (5'→3')	Product size, bp
Caspase-3	F: TGGTGATGAAGGGGTCATTTATG	105
	R: TTCGGCTTTCCAGTCAGACTC	
Caspase-9	F: TCCTGGTACATCGAGACCTTG	109
	R: AAGTCCCTTTCGCAGAAACAG	
Bcl-2	F: GCTACCGTCGTGACTTCGC	147
	R: CCCCACCGAACTCAAAGAAGG	
Bax	F: TGAAGACAGGGGCCTTTTTG	140
	R: AATTCGCCGGAGACACTCG	
ANP	F: GCTTCCAGGCCATATTGGAG	126
	R: GGGGGCATGACCTCATCTT	
BNP	F: GAGGTCACTCCTATCCTCTGG	100
	R: GCCATTTCCTCCGACTTTTCTC	
α-MHC	F: TGAGTGGGAGTTTATCGACTTCG	194
	R: CCTTGACATTGCGAGGCTTC	
β-MHC	F: CCTGCGGAAGTCTGAGAAGG	119
	R: CTCGGGACACGATCTTGGC	
18s	F: CATGCAGAACCCACGACAGTA	119
	R: CCTCACGCAGCTTGTTGTCTA	

ANP, atrial natriuretic peptide; BNP, brain natriuretic peptide; α-MHC, α-myosin heavy chain; β-MHC, β-myosin heavy chain; F, forward; R, reverse.

complex (Sigma-Aldrich; Merck KGaA) at 37˚C overnight. Following washing in Tris buffer, sections were counterstained with hematoxylin at 25˚C for 2 min and washed again in Tris buffer. In total, five visual fields were randomly selected in each group to observe the apoptosis under a light microscope (BX53; Olympus Corporation; magnification, x200). The results were quantified using Image-Pro Plus software (version 6.0; Media Cybernetics, Inc.).

Reverse transcription-quantitative PCR (RT-qPCR). Total RNA was extracted from heart tissues using TRIzol® reagent (Invitrogen; Thermo Fisher Scientific, Inc.). Total RNA purity and concentration were assessed using a Nanodrop 2000 Spectrophotometer (Thermo Fisher Scientific, Inc.). Total RNA (1 µg) was reverse transcribed into cDNA using PrimeScript RT MasterMix (37˚C for 15 min; 85˚C for 5 sec, held at 4˚C; Takara Biotechnology Co., Ltd.). Subsequently, qPCR was performed to measure the mRNA expression levels of atrial natriuretic peptide (ANP), brain natriuretic peptide (BNP), α-myosin heavy polypeptide (MHC), β-MHC, Bcl-2, Bax, caspase-3, caspase-9 and 18s using a CFX-96 Touch Thermocycler PCR system and SYBR Green Master Mix. The thermocycling conditions used for qPCR were as follows: Initial denaturation at 94˚C for 30 sec, followed by 45 cycles of 94˚C for 5 sec, 58˚C for 30 sec and 72˚C for 30 sec, then a dissociation stage (95˚C for 15 sec, 65˚C for 30 sec and 95˚C for 15 sec). The sequences of the primers used for qPCR are listed in Table I. mRNA expression levels were quantified using the $2^{-\Delta\Delta Cq}$ method (33) and normalized to the internal reference gene 18s.

Western blotting. A standard western blotting protocol was used to measure protein expression, as previously described (32). Briefly, cytoplasmic and nuclear proteins were extracted from heart tissues using a protein extraction kit (cat. no. CW0199S; CoWin Bioscience Co., Ltd.). Protein concentrations were measured using a BCA protein quantification kit (CWBio). Proteins (50 µg) were separated via 12% SDS-PAGE and transferred to nitrocellulose membranes. Following blocking in 5% fat-free milk in TBS-0.1% Tween-20 (TBST) for 2 h at room temperature, the membranes were incubated at 4˚C overnight with primary antibodies targeted against: Bcl-2 (1:500; cat. no. sc-7382; Santa Cruz Biotechnology, Inc.), Bax (1:500; cat. no. sc-7480; Santa Cruz Biotechnology, Inc.), cleaved caspase-3 (1:1,000; cat. no. ab214430; Abcam), cleaved caspase-9 (1:1,000; cat. no. 9509; Cell Signaling Technology, Inc.), phosphorylated (p)-Akt (1:1,000; cat. no. 4060; Cell Signaling Technology, Inc.), Akt (1:1,000; cat. no. 9272; Cell Signaling Technology, Inc.), Nrf2 (1:500; cat. no. sc-13032; Santa Cruz Biotechnology, Inc.), HO-1 (1:1,000; cat. no. ab68477; Abcam), NAD(P)H quinone oxidoreductase-1 (NQO-1; 1:500; cat. no. sc-32793; Santa Cruz Biotechnology, Inc.), γ-GCS (1:500; cat. no. sc-166603; Santa Cruz Biotechnology, Inc.), lamin B1 (1:500; cat. no. sc-374015; Santa Cruz Biotechnology, Inc.) and β-actin (1:1,000; cat. no. CW0096M; CWBio). Following washing with TBST, the membranes were incubated with a HRP-conjugated secondary antibody (1:10,000; anti-rabbit IgG, cat. no. 31460 or anti-mouse IgG, cat. no. 31430; Thermo Fisher Scientific, Inc.) at room temperature for 2 h. Protein bands were visualized using SuperSignal™ West Pico PLUS chemiluminescent substrate (cat. no. 34580; Thermo Fisher Scientific, Inc.). Protein expression was semi-quantified using Image Lab
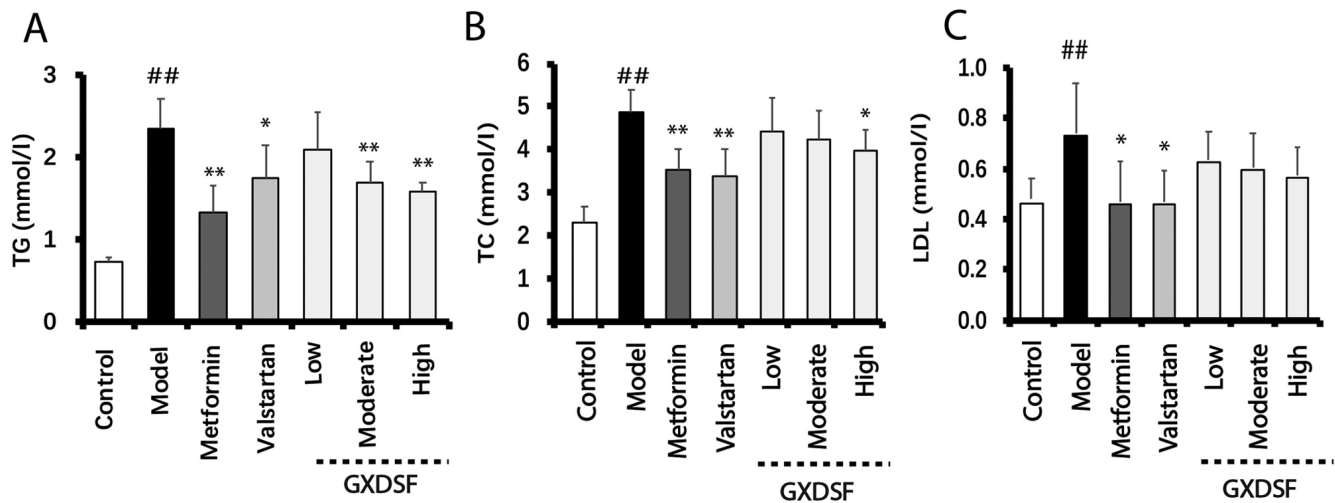
Figure 2. Effects of GXDSF on serum lipid levels in *db/db* mice. Serum (A) TG, (B) TC and (C) LDL levels in each group. Data are expressed as the mean ± SD (n =10). ##P<0.01 vs. control; *P<0.05 and **P<0.01 vs. model. GXDSF, Guan Xin Dan Shen formulation; TG, triglyceride; TC, total cholesterol; LDL, low-density lipoprotein cholesterol.

software (version 3.0; Bio-Rad Laboratories, Inc.). β-actin and lamin B1 were used as the loading controls for cytoplasmic and nuclear proteins, respectively.

Statistical analysis. All experiments were performed ≥3 times. Data are presented as the mean ± SD. Statistical analyses were performed using SPSS software (version 19.0; IBM Corp.). Comparisons among multiple groups were analyzed using one-way or mixed two-way ANOVA follow by Tukey's post hoc test. P<0.05 was considered to indicate a statistically significant difference.

Results

GXDSF reduces the increase in body weight and enhances insulin sensitivity in db/db mice. The body weight of *db/db* mice was measured over the 10-week treatment period. Compared with the model group, the body weight of the mice in the GXDSF high-dose groups was reduced, but this trend was not significant (Fig. 1B). Compared with the model group, metformin significantly decreased elevated FBG levels in *db/db* mice (P<0.05; Fig. 1C), whereas the effect of GXDSF on FBG was not significant compared with the model group, which suggested that GXDSF displayed no distinct hypoglycemic effect in *db/db* mice. Subsequently, insulin sensitivity following GXDSF treatment was assessed. The ITT results demonstrated that both moderate- and high-dose GXDSF enhanced insulin sensitivity, as indicated by significantly decreased AUC values compared with the model group (P<0.01; Fig. 1D and E).

GXDSF decreases serum lipid levels in db/db mice. Compared with the control group, *db/db* mice displayed significantly increased serum lipid levels in the model group (Fig. 2). Administration of metformin or high-dose GXDSF significantly reduced serum TG and TC levels in *db/db* mice compared with the model group (P<0.05; Fig. 2A and B). Additionally, increased serum LDL levels in *db/db* mice were

significantly reduced by metformin or valsartan administration compared with the model group (both P<0.05; Fig. 2C). Serum LDL levels in the GXDSF groups were slightly reduced, but the differences were not significant compared with the model group.

GXDSF ameliorates the cardiac dysfunction of db/db mice. After 10 weeks of GXDSF treatment, M-mode echocardiography was used to assess cardiac function. Compared with the control group, *db/db* mice in the model group displayed a significantly larger LVIDd (Fig. 3A). Administration of valsartan or high-dose GXDSF significantly reduced LVIDd compared with the model group (P<0.01). Compared with the model group, the effects of metformin and moderate- and low-dose GXDSF on the LVIDd and LVIDs were not significant (Fig. 3B and C). Additionally, compared with the control group, the LV end-systolic volume and LV end-diastolic volume of the *db/db* mice in the model group were significantly reduced (P<0.01), whereas valsartan, moderate-dose GXDSF and high-dose GXDSF treatment significantly increased these volumes in *db/db* mice (P<0.05; Fig. S1A and B). Additionally, compared with the model group, valsartan or GXDSF treatment significantly improved the impaired left ventricular EF and FS in *db/db* mice (P<0.05; Fig. 3D and E).

GXDSF attenuates diabetes-induced cardiac hypertrophy in db/db mice. After GXDSF treatment, the heart weight was initially measured. Compared with the control group, the heart weight of the model group was significantly increased, which was significantly reduced by treatment with metformin, moderate-dose GXDSF or high-dose GXDSF (P<0.05; Fig. 4A and B). In the model group, the *db/db* mice developed notable myocardial hypertrophy, as evidenced by H&E staining, which demonstrated disordered cardiac fibers (Fig. 4C). However, compared with the model group, treatment with metformin or GXDSF for 10 weeks markedly reduced myocardial hypertrophy in *db/db* mice. Moreover, compared with the control group, the mRNA expression levels of cardiac
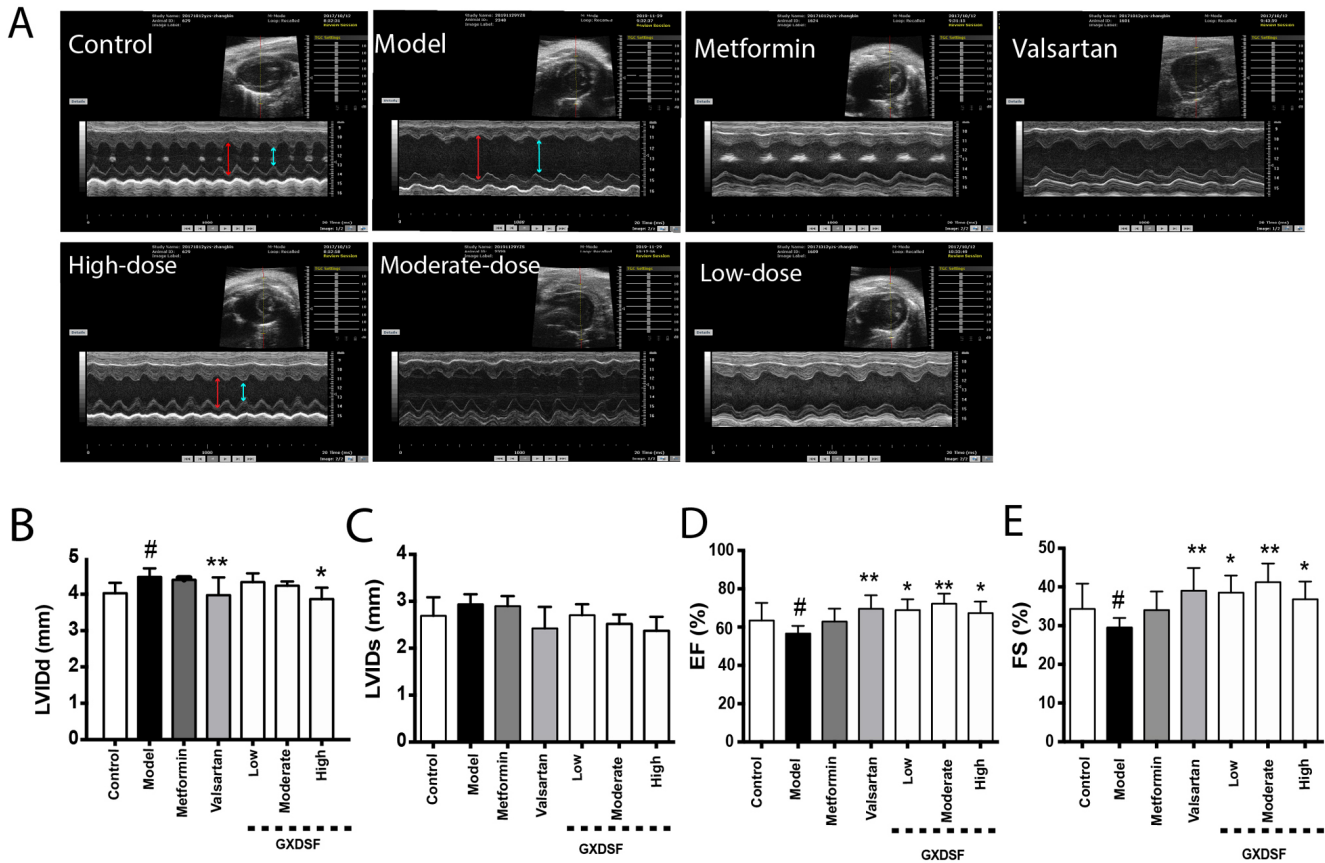
Figure 3. Effects of GXDSF on the cardiac function of *db/db* mice. (A) Echocardiograms were obtained via echocardiography. (B) LVIDd, (C) LVIDs, (D) % EF and (E) % FS. Data are presented as the mean ± SD (n=5). #P<0.05 vs. control; *P<0.05 and **P<0.01 vs. model. GXDSF, Guan Xin Dan Shen formulation; LVIDd, left ventricular end diastolic diameter; LVIDs, left ventricular end systolic diameter; % EF, percentage ejection fraction; % FS, percentage fractional shortening.

hypertrophy-related genes ANP, BNP and β-MHC/α-MHC were significantly increased in the heart tissues of the model group (P<0.01), which was significantly reversed by treatment with metformin, valsartan or GXDSF (P<0.05; Fig. 4D). Furthermore, treatment with moderate- or high-dose GXDSF significantly decreased the serum levels of CK-MB and LDH compared with the model group (Fig. 4E). Additionally, high-dose GXDSF could reduce the increased serum AST level. Collectively, the aforementioned results indicated that GXDSF prevented diabetes-induced cardiac hypertrophy.

GXDSF attenuates diabetes-induced cardiomyocyte apoptosis in db/db mice. Diabetes-induced cardiomyocyte apoptosis is closely associated with cardiac hypertrophy (34). The TUNEL assay results demonstrated that there was a significantly higher proportion of apoptotic cells in the hearts of the model mice compared with the control group (Fig. 5A and B). After 10 weeks of treatment with metformin or GXDSF, the ratio of apoptotic cells was notably decreased. The mRNA and protein expression levels of apoptosis-related markers were further examined. In line with the results of the TUNEL assay, compared with the model group, GXDSF significantly decreased the mRNA expression levels of Bax, caspase-3 and caspase-9 (Fig. 5D and E), but significantly upregulated the mRNA expression levels of Bcl-2 (Fig. 5C). The western blotting results revealed that the Bcl-2/Bax ratio

significantly decreased, whereas the protein expression levels of cleaved caspase-3 and cleaved caspase-9 were significantly upregulated in the heart tissues of *db/db* mice in the model group compared with the control group (Fig. 5G-I). Diabetes-induced alterations in protein expression were significantly reversed by GXDSF treatment (Fig. 5G-I), indicating that GXDSF protected the diabetic heart against apoptosis.

GXDSF promotes translocation of Nrf2 to the nucleus to increase the expression of antioxidant enzymes. The PI3K/Akt signaling pathway and Nrf2-mediated antioxidant enzymes serve key anti-apoptotic roles (35), and our previous study demonstrated that GXDSF increased Akt phosphorylation (22). Therefore, it was hypothesized that GXDSF may protect against diabetes-induced cardiomyocyte apoptosis by increasing Akt phosphorylation and Nrf2 signaling. The western blotting results demonstrated that Akt phosphorylation, Nrf2 nuclear translocation and the expression of antioxidant enzymes (γ-GCS, NQO-1 and HO-1) were significantly decreased in the heart tissues of *db/db* mice in the model group compared with the control group (Fig. 6A-F). After treatment with GXDSF, the expression levels of p-Akt, nuclear Nrf2, HO-1 and NQO-1 were significantly upregulated compared with the model group. The results suggested that GXDSF promoted Akt and Nrf2 signaling,
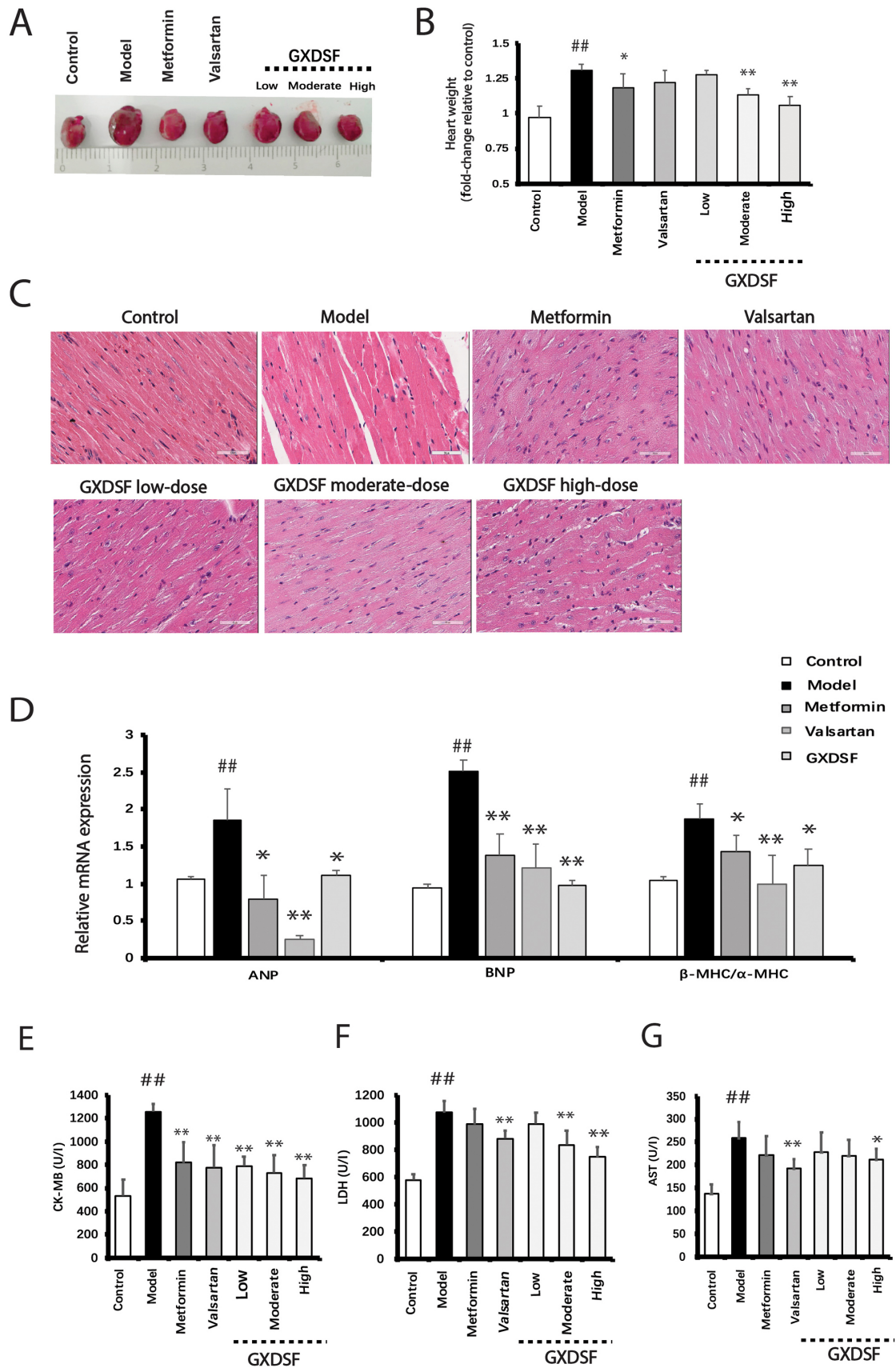
Figure 4. Effect of GXDSF on pathological alterations to the heart in *db/db* mice. (A) Representative images of hearts isolated from *db/db* mice in each group. (B) Heart weight of *db/db* mice in each group. (C) Representative images of hematoxylin and eosin staining for identification of the pathological structure of the heart (n=5; scale bar, 50 *μ*m). (D) Reverse transcription-quantitative PCR was performed to measure the impact of GXDSF (high-dose) on the mRNA expression levels of cardiac hypertrophy-related genes. Serum (E) CK-MB, (F) LDH and (G) AST levels in *db/db* mice. Data are presented as the mean ± SD (n=10). ##P<0.01 vs. control; *P<0.05 and **P<0.01 vs. model. GXDSF, Guan Xin Dan Shen formulation; CK-MB, creatine kinase MB; LDH, lactate dehydrogenase; AST, aspartate transaminase; ANP, atrial natriuretic peptide; BNP, brain natriuretic peptide; α-MHC, α-myosin heavy chain; β-MHC, β-myosin heavy chain.
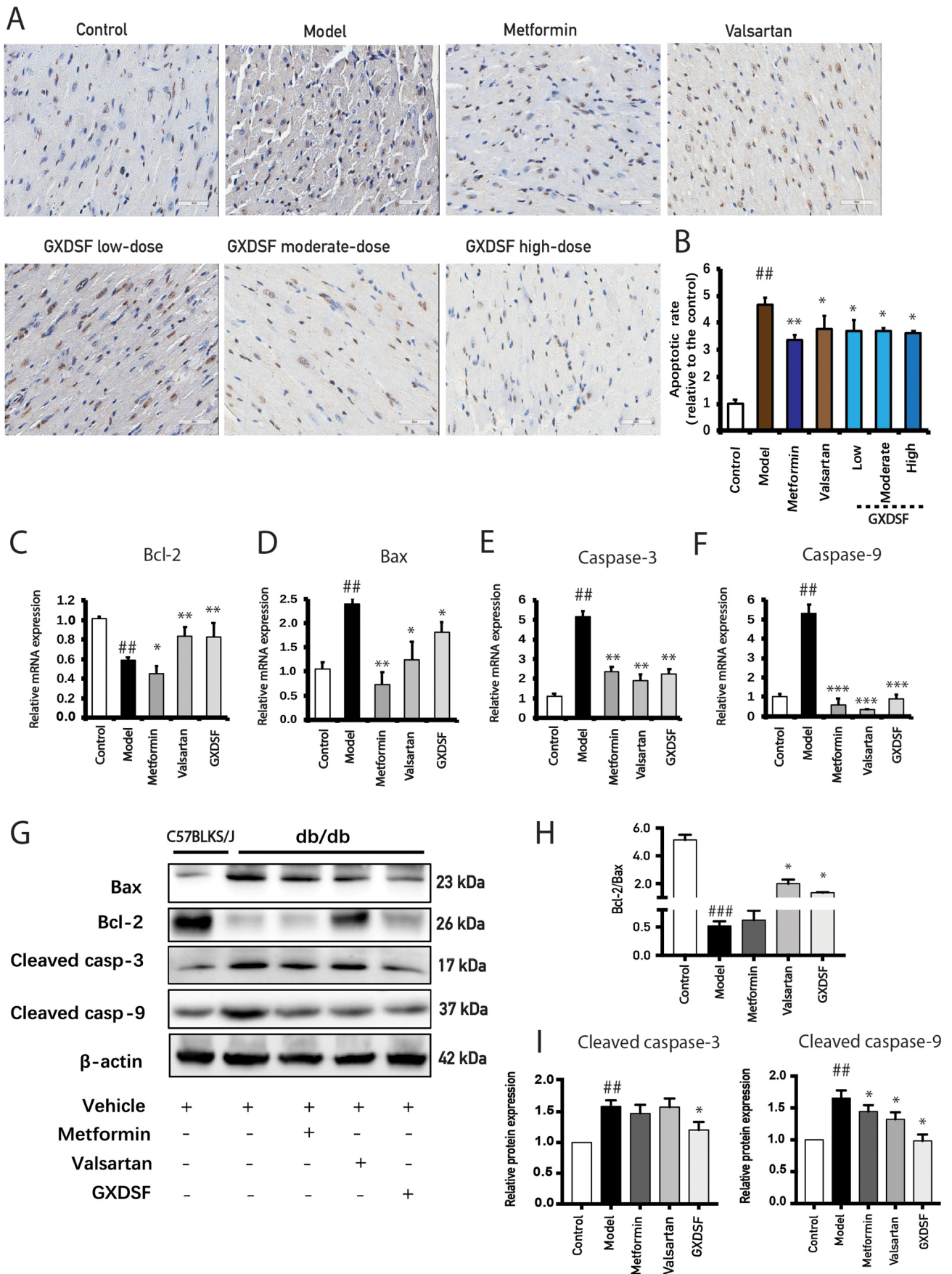
Figure 5. Effect of GXDSF on cardiac apoptosis in each group. Cardiac apoptosis was (A) determined by performing TUNEL staining (magnification, x200; scale bar, 50 μm) and (B) quantified in each group (n=5). Reverse transcription-quantitative PCR was performed to measure the impact of GXDSF (high-dose) on the mRNA expression of apoptosis-related genes, including (C) Bcl-2, (D) Bax, (E) caspase-3 and (F) caspase-9 (n=10). Protein expression levels were (G) determined via western blotting and semi-quantified for (H) Bcl-2/Bax, (I) cleaved caspase-3 and cleaved caspase-9 (n=3). Data are presented as the mean ± SD. ##P<0.01 and ###P<0.001 vs. control; *P<0.05, **P<0.01 and ***P<0.001 vs. model. GXDSF, Guan Xin Dan Shen formulation.
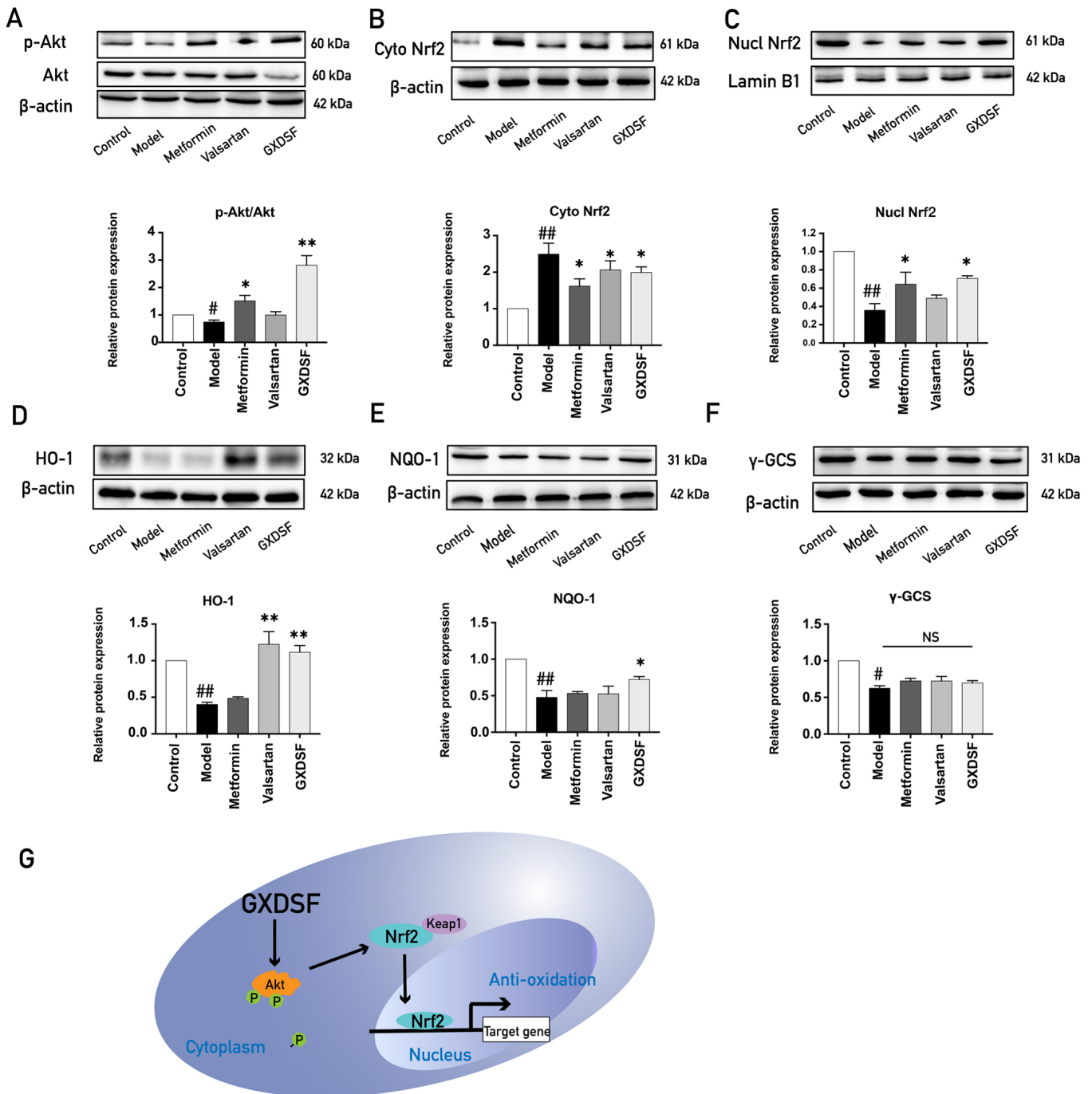
Figure 6. GXDSF-induced activation of the Akt-mediated Nrf2 signaling pathway. Western blotting was performed to determine the impact of high dose of GXDSF on the protein expression of (A) p-Akt, (B) cytoplasmic Nrf2, (C) nuclear Nrf2, (D) HO-1, (E) NQO-1 and (F) γ-GCS (n=3). (G) Schematic illustration indicating the mechanism underlying the protective effects of GSDXF against diabetic cardiomyopathy. Data are presented as the mean ± SD. #P<0.05 and ##P<0.01 vs. control; *P<0.05 and **P<0.01 vs. model. GXDSF, Guan Xin Dan Shen formulation; p, phosphorylated; Nrf2, nuclear factor-erythroid 2-related factor 2; HO-1, heme oxygenase-1; γ-GCS, γ-glutamylcysteine synthetase heavy subunit; NQO-1, NAD(P)H quinone oxidoreductase-1; NS, not significant; cyto, cytoplasmic; nucl, nuclear; Keap1, kelch like ECH associated protein.

which subsequently upregulated the expression of antioxidant enzymes (Fig. 6G).

Discussion

With an increasing prevalence of diabetes worldwide, the incidence of DCM is also becoming an increasingly more common problem. DCM is characterized by myocardial left ventricular dysfunction, cardiac injury, cardiomyocyte hypertrophy, cardiomyocyte apoptosis and microvascular abnormalities (36,37), which may be the result of hyperglycemia, oxidative stress, Ca²⁺ overload, ischemia and hypoxia (24,38,39). According to previous studies, LV diastolic dysfunction is closely related to myocardial cell apoptosis, and inhibition of apoptosis may improve cardiac function (40). Increased myocardial cell apoptosis leads to loss of contractile units and cardiac remodeling, which ultimately results in cardiac dysfunction (41,42). The present

study demonstrated that GXDSF may prevent the development of DCM by enhancing insulin sensitivity, decreasing diabetic heart weight, improving cardiac function and inhibiting cardiac hypertrophy. Mechanistically, the results indicated that GXDSF may exert cardioprotective effects via Akt/Nrf2-mediated upregulation of antioxidant enzymes. Therefore, the present study suggested that GXDSF may serve as a therapeutic agent for the prevention of DCM.

Chronic hyperglycemia, hyperlipidemia and insulin resistance collectively lead to the development of DCM (43-45). These risk factors not only result in metabolic dysfunction, but also in severe oxidative stress and mitochondrial injury (46,47). Currently, both *db/db* mice and streptozotocin (STZ) with high-fat diet-induced mice are used as models of diabetes, and each model displays different characteristics. The STZ with high-fat diet-induced mouse model is more economical, but STZ might have some unknown impacts on the mice. Another problem of the STZ with high-fat diet-induced model is that the fasting blood glucose is not as stable compared with *db/db* mice (48). The majority of previous studies investigating DCM used *db/db* mice as a model of DCM (49,50). Therefore, the present study selected *db/db* mice as a model to study the protective effect of GXDSF. Metformin was selected as a positive control for examining the hyperglycemic effects of GXDSF. Compared with the model group, the effect of GXDSF on FBG was insignificant; however, moderate and high doses of GXDSF significantly improved insulin sensitivity and decreased serum TG levels. The antilipemic effects of GXDSF may be related to *notoginseng*, a key component of GXDSF that is closely associated with fat metabolism according to recent studies (51,52).

Mitochondria are crucial organelles that mediate cardiomyocyte apoptosis (53). Loss of the mitochondrial membrane potential is a key step in activating mitochondrial-mediated apoptosis, which is primarily controlled by the Bcl-2 family of proteins (54), vital mediators of apoptosis (55). Mitochondrial permeability is regulated by Bcl-2 and Bax (56). An increase in the Bax/Bcl-2 ratio results in release of cytochrome *c* and activation of caspase-3, leading to apoptosis (57). Compared with the model group, GXDSF treatment significantly reduced the expression levels of the proapoptotic protein Bax, increased the expression of the antiapoptotic protein Bcl-2, and reduced the protein expression levels of cleaved caspase-3 and cleaved caspase-9. Collectively, the aforementioned results demonstrated that GXDSF inhibited metabolic dysfunction-mediated cardiomyocyte apoptosis.

Numerous stimuli, including hypoxia, oxidative stress and mechanical stress, can activate the PI3K/Akt signaling pathway (58). Activation of Akt signaling is sufficient to inhibit cardiomyocyte apoptosis and maintain the function of viable cardiomyocytes (59). Promoting Akt signaling inhibits high glucose-induced cardiomyocyte apoptosis (60). Consistent with the aforementioned studies, the present study demonstrated that GXDSF significantly upregulated p-Akt in the diabetic heart of *db/db* mice compared with the model group. Cytoplasmic Nrf2 separates with kelch like ECH associated protein and subsequently enters into the nucleus to participate in controlling gene expressions. Our previous study demonstrated that upregulation of p-Akt expression promoted Nrf2-mediated expression of HO-1 and NQO-1 (61),

an endogenic antioxidant enzyme with anti-apoptotic and anti-inflammatory properties (62). As GXDSF can regulate p-Akt expression, it was hypothesized that it may increase HO-1 expression by regulating translocation of Nrf2. In the present study, compared with the control group, a significant increase in the cytoplasmic protein expression levels of Nrf2 and a significant decrease in the nuclear protein expression levels of Nrf2 in the diabetic heart of model mice was observed, suggesting that Nrf2 nuclear translocation was inhibited. Furthermore, the results indicated that GXDSF facilitated the nuclear translocation of Nrf2, reversing the downregulation of the expression levels of the antioxidant enzymes HO-1 and NQO-1 in *db/db* mice.

The present study preferentially evaluated the protective effects of GXDSF on DCM in *db/db* mice because 90% of cases of diabetes are type 2 DM (63). However, the present study did not investigate whether GXDSF attenuated the progression of DCM in type 1 DM. Cardiac hypertrophy and fibrosis serve key roles in DCM (64). However, diabetes-induced cardiac hypertrophy and myocardial fibrosis appeared in different periods of DCM (65). The impact of GXDSF on diabetes-induced myocardial fibrosis is not completely understood. Moreover, to further clarify the exact mechanism underlying GXDSF-mediated prevention of DCM, future studies should utilize a H9c2 cell model with or without Nrf2 knockdown.

In conclusion, to the best of our knowledge, the present study was the first to demonstrate the protective function of GXDSF against DCM via upregulation of Nrf2-mediated antioxidant enzyme expression. The results of the present study highlighted the potential therapeutic properties of GXDSF for the management of DCM and glucose control.

Availability of data and materials

The datasets used and/or analyzed during the current study are available from the corresponding author on reasonable request.

Authors' contributions

XBS and GBS contributed to the conception and design of the present study. BZ, CYZ and XLZ performed the experiments. CYZ participated in performing the histological and western blotting procedures. XLZ collected the data and performed statistical analyses. BZ drafted the manuscript. BZ and XBS confirmed the authenticity of all the raw data. All authors read and approved the final version of the manuscript.

Ethics approval and consent to participate

The animal experiments were approved by the Laboratory Animal Ethics Committee of the Institute of Medicinal Plant Development, Peking Union Medical College and Chinese Academy of Medical Sciences (license no. SLXD-20190406017).

Patient consent for publication

Not applicable.

Competing interests

The authors declare that they have no competing interests.

References

1. Barooti A, Kamran M, Kharazmi F, Eftakhar E, Malekzadeh K, Talebi A and Soltani N: Effect of oral magnesium sulfate administration on blood glucose hemostasis via inhibition of gluconeogenesis and FOXO1 gene expression in liver and muscle in diabetic rats. Biomed Pharmacother 109: 1819-1825, 2019.
2. Perry BD, Caldow MK, Brennan-Speranza TC, Sbaraglia M, Jerums G, Garnham A, Wong C, Levinger P, Asrar Ul Haq M, Hare DL, et al: Muscle atrophy in patients with type 2 diabetes mellitus: Roles of inflammatory pathways, physical activity and exercise. Exerc Immunol Rev 22: 94-109, 2016.
3. Papatheodorou K, Banach M, Bekiari E, Rizzo M and Edmonds M: Complications of diabetes 2017. J Diabetes Res 2018: 3086167, 2018.
4. Tsai TH, Lin CJ, Chua S, Chung SY, Chen SM, Lee CH and Hang CL: Deletion of RasGRF1 attenuated interstitial fibrosis in streptozotocin-induced diabetic cardiomyopathy in mice through affecting inflammation and oxidative stress. Int J Mol Sci 19: 3094, 2018.
5. Lam CS: Diabetic cardiomyopathy: An expression of stage B heart failure with preserved ejection fraction. Diab Vasc Dis Res 12: 234-238, 2015.
6. Dai B, Li H, Fan J, Zhao Y, Yin Z, Nie X, Wang DW and Chen C: MiR-21 protected against diabetic cardiomyopathy induced diastolic dysfunction by targeting gelsolin. Cardiovasc Diabetol 17: 123, 2018.
7. Ni R, Cao T, Xiong S, Ma J, Fan GC, Lacefield JC, Lu Y, Le Tissier S and Peng T: Therapeutic inhibition of mitochondrial reactive oxygen species with mito-TEMPO reduces diabetic cardiomyopathy. Free Radic Biol Med 90: 12-23, 2016.
8. Luo W, Jin Y, Wu G, Zhu W, Qian Y, Zhang Y, Li J, Zhu A and Liang G: Blockage of ROS and MAPKs-mediated inflammation via restoring SIRT1 by a new compound LF10 prevents type 1 diabetic cardiomyopathy. Toxicol Appl Pharmacol 370: 24-35, 2019.
9. Kayama Y, Raaz U, Jagger A, Adam M, Schellinger IN, Sakamoto M, Suzuki H, Toyama K, Spin JM and Tsao PS: Diabetic cardiovascular disease induced by oxidative stress. Int J Mol Sci 16: 25234-25263, 2015.
10. Wang J, Song Y, Elsherif L, Song Z, Zhou G, Prabhu SD, Saari JT and Cai L: Cardiac metallothionein induction plays the major role in the prevention of diabetic cardiomyopathy by zinc supplementation. Circulation 113: 544-554, 2006.
11. Wu MS, Liang JT, Lin YD, Wu ET, Tseng YZ and Chang KC: Aminoguanidine prevents the impairment of cardiac pumping mechanics in rats with streptozotocin and nicotinamide-induced type 2 diabetes. Br J Pharmacol 154: 758-764, 2008.
12. Lu J, Pontré B, Pickup S, Choong SY, Li M, Xu H, Gamble GD, Phillips AR, Cowan BR, Young AA and Cooper GJ: Treatment with a copper-selective chelator causes substantive improvement in cardiac function of diabetic rats with left-ventricular impairment. Cardiovasc Diabetol 12: 28, 2013.
13. Forcheron F, Basset A, Abdallah P, Del Carmine P, Gadot N and Beylot M: Diabetic cardiomyopathy: Effects of fenofibrate and metformin in an experimental model-the Zucker diabetic rat. Cardiovasc Diabetol 8: 16, 2009.
14. Xie Z, Lau K, Eby B, Lozano P, He C, Pennington B, Li H, Rathi S, Dong Y, Tian R, et al: Improvement of cardiac functions by chronic metformin treatment is associated with enhanced cardiac autophagy in diabetic OVE26 mice. Diabetes 60: 1770-1778, 2011.
15. Rösen R, Rump AF and Rösen P: The ACE-inhibitor captopril improves myocardial perfusion in spontaneously diabetic (BB) rats. Diabetologia 38: 509-517, 1995.
16. Al-Shafei AI, Wise RG, Gresham GA, Bronns G, Carpenter TA, Hall LD and Huang CL: Non-invasive magnetic resonance imaging assessment of myocardial changes and the effects of angiotensin-converting enzyme inhibition in diabetic rats. J Physiol 538: 541-553, 2002.
17. Turan B: A comparative summary on antioxidant-like actions of timolol with other antioxidants in diabetic cardiomyopathy. Curr Drug Deliv 13: 418-423, 2016.
18. Savarese G, D'Amore C, Federici M, De Martino F, Dellegrottaglie S, Marciano C, Ferrazzano F, Losco T, Lund LH, Trimarco B, et al: Effects of dipeptidyl peptidase 4 inhibitors and sodium-glucose linked coTransporter-2 inhibitors on cardiovascular events in patients with type 2 diabetes mellitus: A meta-analysis. Int J Cardiol 220: 595-601, 2016.
19. Suzuki T and Yamamoto M: Molecular basis of the Keap1-Nrf2 system. Free Radic Biol Med 88: 93-100, 2015.
20. Ge ZD, Lian Q, Mao X and Xia Z: Current status and challenges of NRF2 as a potential therapeutic target for diabetic cardiomyopathy. Int Heart J 60: 512-520, 2019.
21. Luo J, Yan D, Li S, Liu S, Zeng F, Cheung CW, Liu H, Irwin MG, Huang H and Xia Z: Allopurinol reduces oxidative stress and activates Nrf2/p62 to attenuate diabetic cardiomyopathy in rats. J Cell Mol Med 24: 1760-1773, 2020.
22. Deng X, Xing X, Sun G, Xu X, Wu H, Li G and Sun X: Guanxin danshen formulation protects against myocardial ischemia reperfusion injury-induced left ventricular remodeling by upregulating estrogen receptor β. Front Pharmacol 8: 777, 2017.
23. Li J, Han L, Zhu, Wang D, Shang Z: Guanxin Danshen Pills in Treatment of 200 Cases of Patients with Coronary Heart Disease Angina Pectoris. China &Foreign Medical Treatment 24: 126-128, 2017.
24. Yu Y, Sun G, Luo Y, Wang M, Chen R, Zhang J, Ai Q, Xing N and Sun X: Cardioprotective effects of Notoginsenoside R1 against ischemia/reperfusion injuries by regulating oxidative stress- and endoplasmic reticulum stress- related signaling pathways. Sci Rep 6: 21730, 2016.
25. Xiao J, Zhu T, Yin YZ and Sun B: Notoginsenoside R1, a unique constituent of Panax notoginseng, blinds proinflammatory monocytes to protect against cardiac hypertrophy in ApoE$^{-/-}$ mice. Eur J Pharmacol 833: 441-450, 2018.
26. Fan C, Qiao Y and Tang M: Notoginsenoside R1 attenuates high glucose-induced endothelial damage in rat retinal capillary endothelial cells by modulating the intracellular redox state. Drug Des Devel Ther 11: 3343-3354, 2017.
27. Yu LJ, Zhang KJ, Zhu JZ, Zheng Q, Bao XY, Thapa S, Wang Y and Chu MP: Salvianolic acid exerts cardioprotection through promoting angiogenesis in animal models of acute myocardial infarction: Preclinical evidence. Oxid Med Cell Longev 2017: 8192383, 2017.
28. Yu H, Zhen J, Yang Y, Gu J, Wu S and Liu Q: Ginsenoside Rg1 ameliorates diabetic cardiomyopathy by inhibiting endoplasmic reticulum stress-induced apoptosis in a streptozotocin-induced diabetes rat model. J Cell Mol Med 20: 623-631, 2016.
29. Paolillo S, Marsico F, Prastaro M, Renga F, Esposito L, De Martino F, Di Napoli P, Esposito I, Ambrosio A, Ianniruberto M, et al: Diabetic cardiomyopathy: Definition, diagnosis, and therapeutic implications. Heart Fail Clin 15: 341-347, 2019.
30. National Research Council (US) Institute for Laboratory Animal Research: Guide for the Care and Use of Laboratory Animals. National Academies Press, Washington, DC, 1996.
31. Xie W, Meng X, Zhai Y, Ye T, Zhou P, Nan F, Sun G and Sun X: Antidepressant-like effects of the Guanxin Danshen formula via mediation of the CaMK II-CREB-BDNF signalling pathway in chronic unpredictable mild stress-induced depressive rats. Ann Transl Med 7: 564, 2019.
32. Shan T, Liang X, Bi P and Kuang S: Myostatin knockout drives browning of white adipose tissue through activating the AMPK-PGC1α-Fndc5 pathway in muscle. FASEB J 27: 1981-1989, 2013.
33. Livak KJ and Schmittgen TD: Analysis of relative gene expression data using real time quantitative PCR and the 2(-Delta Delta C(T)) method. Methods 25: 402-408, 2001.

34. Zhang C, Wang F, Zhang Y, Kang Y, Wang H, Si M, Su L, Xin X, Xue F, Hao F, *et al*: Celecoxib prevents pressure overload-induced cardiac hypertrophy and dysfunction by inhibiting inflammation, apoptosis and oxidative stress. J Cell Mol Med 20: 116-127, 2016.
35. Chai C, Song LJ, Han SY, Li XQ and Li M: MicroRNA-21 promotes glioma cell proliferation and inhibits senescence and apoptosis by targeting SPRY1 via the PTEN/PI3K/AKT signaling pathway. CNS Neurosci Ther 24: 369-380, 2018.
36. Wang S, Zhang T, Yang Z, Lin J, Cai B, Ke Q, Lan W, Shi J, Wu S and Lin W: Heme oxygenase-1 protects spinal cord neurons from hydrogen peroxide-induced apoptosis via suppression of Cdc42/MLK3/MKK7/JNK3 signaling. Apoptosis 22: 449-462, 2017.
37. Huynh K, Bernardo BC, McMullen JR and Ritchie RH: Diabetic cardiomyopathy: Mechanisms and new treatment strategies targeting antioxidant signaling pathways. Pharmacol Ther 142: 375-415, 2014.
38. Boudina S, Bugger H, Sena S, O'Neill BT, Zaha VG, Ilkun O, Wright JJ, Mazumder PK, Palfreyman E, Tidwell TJ, *et al*: Contribution of impaired myocardial insulin signaling to mitochondrial dysfunction and oxidative stress in the heart. Circulation 119: 1272-1283, 2009.
39. Dludla PV, Joubert E, Muller CJF, Louw J and Johnson R: Hyperglycemia-induced oxidative stress and heart disease-cardioprotective effects of rooibos flavonoids and phenylpyruvic acid-2-O-β-D-glucoside. Nutr Metab (Lond) 14: 45, 2017.
40. Gencoglu H, Tuzcu M, Hayirli A and Sahin K: Protective effects of resveratrol against streptozotocin-induced diabetes in rats by modulation of visfatin/sirtuin-1 pathway and glucose transporters. Int J Food Sci Nutr 66: 314-320, 2015.
41. Zhu R, Sun H, Yu K, Zhong Y, Shi H, Wei Y, Su X, Xu W, Luo Q, Zhang F, *et al*: Interleukin-37 and dendritic cells treated with interleukin-37 plus troponin I ameliorate cardiac remodeling after myocardial infarction. J Am Heart Assoc 5: e004406, 2016.
42. Zhang WX, He BM, Wu Y, Qiao JF and Peng ZY: Melatonin protects against sepsis-induced cardiac dysfunction by regulating apoptosis and autophagy via activation of SIRT1 in mice. Life Sci 217: 8-15, 2019.
43. Yamada S, Ding Y, Tanimoto A, Wang KY, Guo X, Li Z, Tasaki T, Nabesima A, Murata Y, Shimajiri S, *et al*: Apoptosis signal-regulating kinase 1 deficiency accelerates hyperlipidemia-induced atheromatous plaques via suppression of macrophage apoptosis. Arterioscler Thromb Vasc Biol 31: 1555-1564, 2011.
44. Guo Y, Yin HJ and Shi DZ: Effect of xinnao shutong capsule on cardiac muscle cell apoptosis and protein expressions of Bcl-2 and Bax in hyperlipidemia rats after myocardial infarction. Zhongguo Zhong Xi Yi Jie He Za Zhi 26: 541-544, 2006 (In Chinese).
45. Wang Y, Xue J, Li Y, Zhou X, Qiao S and Han D: Telmisartan protects against high glucose/high lipid-induced apoptosis and insulin secretion by reducing the oxidative and ER stress. Cell Biochem Funct 37: 161-168, 2019.
46. Giacco F and Brownlee M: Oxidative stress and diabetic complications. Circ Res 107: 1058-1070, 2010.
47. Vásquez-Trincado C, García-Carvajal I, Pennanen C, Parra V, Hill JA, Rothermel BA and Lavandero S: Mitochondrial dynamics, mitophagy and cardiovascular disease. J Physiol 594: 509-525, 2016.
48. Cheng L, Shen ZF, Sun GB and Sun XB: Advances in diabetic animal models and its application in the traditional Chinese medicine research. Yao Xue Xue Bao 50: 951-958, 2015 (In Chinese).
49. Zhang X and Hao Y: Beneficial effects of echinacoside on diabetic cardiomyopathy in diabetic Db/Db mice. Drug Des Devel Ther 14: 5575-5587, 2020.
50. Wang S, Wang B, Wang Y, Tong Q, Liu Q, Sun J, Zheng Y and Cai L: Zinc prevents the development of diabetic cardiomyopathy in db/db Mice. Int J Mol Sci 18: 580. 2017.
51. Quan LH, Zhang C, Dong M, Jiang J, Xu H, Yan C, Liu X, Zhou H, Zhang H, Chen L, *et al*: Myristoleic acid produced by enterococci reduces obesity through brown adipose tissue activation. Gut 69: 1239-1247, 2020.
52. Xu Y, Wang N, Tan HY, Li S, Zhang C, Zhang Z and Feng Y: *Panax notoginseng* saponins modulate the gut microbiota to promote thermogenesis and beige adipocyte reconstructionvia leptin-mediated AMPKα/STAT3 signaling in diet-induced obesity. Theranostics 10: 11302-11323, 2020.
53. Tan PP, Zhou BH, Zhao WP, Jia LS, Liu J and Wang HW: Mitochondria-mediated pathway regulates C2C12 cell apoptosis induced by fluoride. Biol Trace Elem Res 185: 440-447, 2018.
54. Lu Q and Hong W: Bcl2 enhances c-Myc-mediated MMP-2 expression of vascular smooth muscle cells. Cell Signal 21: 1054-1059, 2009.
55. Zhang G, Zeng X, Zhang R, Liu J, Zhang W, Zhao Y, Zhang X, Wu Z, Tan Y, Wu Y and Du B: Dioscin suppresses hepatocellular carcinoma tumor growth by inducing apoptosis and regulation of TP53, BAX, BCL2 and cleaved CASP3. Phytomedicine 23: 1329-1336, 2016.
56. Birkinshaw RW and Czabotar PE: The BCL-2 family of proteins and mitochondrial outer membrane permeabilisation. Semin Cell Dev Biol 72: 152-162, 2017.
57. Antonsson B and Martinou JC: The Bcl-2 protein family. Exp Cell Res 256: 50-57, 2000.
58. Matsui T and Rosenzweig A: Convergent signal transduction pathways controlling cardiomyocyte survival and function: The role of PI 3-kinase and akt. J Mol Cell Cardiol 38: 63-71, 2005.
59. Hong HJ, Liu JC, Chen PY, Chen JJ, Chan P and Cheng TH: Tanshinone IIA prevents doxorubicin-induced cardiomyocyte apoptosis through Akt-dependent pathway. Int J Cardiol 157: 174-179, 2012.
60. Su D, Zhou Y, Hu S, Guan L, Shi C, Wang Q, Chen Y, Lu C, Li Q and Ma X: Role of GAB1/PI3K/AKT signaling high glucose-induced cardiomyocyte apoptosis. Biomed Pharmacother 93: 1197-1204, 2017.
61. Zhang B, Chen Y, Shen Q, Liu G, Ye J, Sun G and Sun X: Myricitrin attenuates high glucose-induced apoptosis through activating Akt-Nrf2 signaling in H9c2 cardiomyocytes. Molecules 21: 880, 2016.
62. Mahalanobish S, Saha S, Dutta S and Sil PC: Mangiferin alleviates arsenic induced oxidative lung injury via upregulation of the Nrf2-HO1 axis. Food Chem Toxicol 126: 41-55, 2019.
63. Unnikrishnan R, Anjana RM and Mohan V: Diabetes mellitus and its complications in India. Nat Rev Endocrinol 12: 357-370, 2016.
64. Athithan L, Gulsin GS, McCann GP and Levelt E: Diabetic cardiomyopathy: Pathophysiology, theories and evidence to date. World J Diabetes 10: 490-510, 2019.
65. Hu X, Bai T, Xu Z, Liu Q, Zheng Y, Cai L: Pathophysiological fundamentals of diabetic cardiomyopathy. Compr Physiol 7: 693-711, 2017.